A decade of technological advances in distributed IP & Resistivity. Why it was needed. What was achieved.

Sharpe, R.[1], Gordon, R.[1], Zhurba, A. [1], Data, E. [1]

1. Quantec Geoscience, Limited

ABSTRACT

Distributed array based technology first gained notoriety in Canada in 2000 with the first demonstration surveys conducted in Ontario with the TITAN 24 DCIP & MT system. Whereas the system boasted "seeing deeper and clearer" than ever before, significant exploration challenges require continued system development. While at the time, this technology definitely led the way for providing deep IP to depths of 750 m, new environments brought new challenges for key items such as resolution, noise suppression and intense digital signal processing.

This paper will summarize the technological advances made to the leading deep imaging distributed IP & resistivity technology over the past decade; culminating in the first full 3D data acquisition electrical surveys for mineral exploration in recent years.

INTRODUCTION

DC Resistivity and IP

In (1953), Dr. David Bleil introduced the mineral exploration world to the IP geophysical technique. In (1959) Dr. Harold Seigel published a mathematical formulation of the effect. Halverson (1967) describes the phase angle concept, methods to defeat EM coupling. Zonge, Sauck and Sumner (1972) describe the similarities and differences of the three fundamental measurement methods. Hallof (1974) began the period where EM coupling could be isolated from phase IP and Pelton et al (1978) include mineral discrimination and the Cole-Cole model in the method. Dey and Morrison (1979) provide the seminal paper on numerical modeling that provides the fundamental basis for array comparison and inversion. In (1981), Halverson et al. introduce the Halverson-Wait model for induced polarization and introduce hybrid time and frequency domain systems. For mineral discrimination, the most useful parameters turn out to be 'tau' in the Cole-Cole and 'R' in the Halverson-Wait models which are both best related to chargeable grain size. In 1994 Oldenburg and Li forever changed the interpretation of electrical data when they introduced an affordable and available inversion code. In a seminal paper for the distributed array system described here John Kingman (1994) introduced digital signal processing (DSP) concepts that would require a paradigm-shift in instrumentation. In a (1998) presentation, Sheard et al. introduced the distributed acquisition system (DAS) with time-series acquisition, current-monitoring, available MT and telluric cancelation. In 1999, John Kingman began working with EMI and Quantec to produce the MT-24 acquisition system and the first survey work was performed in August 2000. TITAN 24 was introduced at PDAC in 2002 and patent licensing was completed in 2003. TITAN 24 is fundamentally designed to acquire array-based MT as well as DC resistivity and IP. Over the next few years, these systems (primarily MIMDAS and TITAN 24) revised the deep exploration paradigm. Goldie (2007) showed the superiority of the methodology for deep IP.

In separate papers, some early work with 3D inversion was published including Collins and White (2003) demonstrated an offset pole-dipole array; and Webb et al (2003) showed the capabilities including building dipoles from a snaking DAS. Gharibi et al (2012) extended the 3D deployment and acquisition paradigm to include a suite of orthogonal dipoles and very high channel count (296) to illustrate the combination of high resolution and deep investigation that was possible. Loke et al (2013) illustrated the capability of 3D software to manage disjointed arrays including a radial distribution. Nyquist (2005) had also concluded that the optimized signal strength of radial data acquisition could produce superior inversion results. Bournas and Thomson (2013) demonstrated the advantage of coupling MT measurements with a 3D omnidirectional acquisition of DC and IP to image an entire porphyry system from the shallow hydrothermal veins though the hypogene and into the porphyry.

Magnetotellurics

The magneto-telluric method was not well-known in the mining business until the introduction of the DAS discussed in this paper. The MT method was first described by Cagniard (1953). Strangway et al (1973) advocate the methods use for mineral exploration while at the same time exposing its many faults in that era (poor instrumentation, poor modeling, limited apparent investigation through conductive overburden). For mining purposes, adding a source (Goldstein and Strangway, 1975) made the method much more useful, albeit interpreted using 1d inversion and near-field correction (Bartel and Jacobson, 1987). Although similarly introduced in 1986 (Wannamaker et al 1987) it wasn't until 2000 that 2D inversion of MT really started to be recognized as superior to CSAMT for the mining business. This may be partly attributed to expected depth of investigation of geophysical methods at the time. Wannamaker and Doerner (2002) provided with an example crossing the Carlin Trend of Nevada the potential value to mineral exploration of mapping to depths of a few km. Still, it wasn't until about 2006 (e.g. Tunser et al. 2006) that publications of the uses of MT in mining became common. Since then, publications like Bournas and Thomson (2013) clearly make the case for the value in augmenting deep imaging (to 500 + m using DCIP for example) with MT investigations that extend mapping to several km.

DISTRIBUTED ARRAY SYSTEMS

DC Resistivity and IP

The state of the art in IP receivers can be summarized as follows, "digital signal processing of time-series acquisition is coupled with monitoring the transmitted current".

The time-series 'revolution' started with John Kingman, MIMDAS, MT-24 and TITAN 24 as described above. These hybrid systems combined the best aspects of the three main technologies of the time, time-domain chargeability, complex resistivity phase (CR) and frequency domain signal comparison (percent frequency effect or PFE). Time-series acquisition means the modern receivers are configured as loggers which fundamentally monitor, by recording a signal sampled at some regular rate, the response of a sensor located at some particular and interesting location within an area of interest. The particular sensors are chosen because they have a measureable response known to be pertinent to the study. Typically these sensors are dipoles of a certain size and orientation sensitive to galvanic measurement of electric field or they are magnetic field measurement devices such as coils. A sampling rate is chosen that is pertinent to the geophysical parameter being measured. For IP signals that are pertinent to the mining community (Macnae 2016) the sampling rate must provide a focus on the band from 'DC' (typically 0.1 Hz) to 50 Hz.

Time-series acquisition implies that the recorded signal will be 'nearly raw' – typically a stream of digitizer counts – and all signal processing will occur separately. This means the signal processing may be repeated as often as necessary to ideally separate the interesting signal from the noise. The signal processing may occur long after the fact – e.g. years in some cases where new methods might improve old results, or immediately for QA/QC purposes. The immediate results may be a pertinent subset of 'quick' methods that provide suitable quality

assurance from, for example, lower-capability processing hardware. The new time-series receivers require much less interface hardware and software than previous receivers because they are not designed to display results, however they require capabilities for massive data storage (up to several GB depending on application) and can benefit from network protocol communication such as LAN or wireless. Some loggers, however, are completely autonomous and data harvest is performed by physically removing or locally downloading the stored data.

Since significant signal processing is not typically included in a logger, these receivers could be considered more 'array independent' than previous receivers. For DC and IP, there may be no attempt to include and calculate geometric factors 'on-the-fly' or internal to the receiver. And similarly for MT, there is no attempt to extract rho and phase. This flexibility comes at the price that it may be difficult to trouble-shoot the sensor associations and location of a receiver. Therefore, modern receivers are capable of 'knowing where they are' via incorporation of a GPS receiver. It should be recognized that in a distributed array shoot, receivers will not typically move. They will remain stationary for a program that may take several days or even a few weeks in the case of a high channel count (300 + receivers) 3D survey. The loggers are usually configured with a battery that permits a minimum 8 hours up-time, but are often capable of running for 24 hours or more. For a distributed system, low channel counts are possible and even desirable. Some receivers are configured with a single channel (e.g. DIAS32, Volterra), others may have 2, 4 or 6 channels (MIMDAS, TITAN 24, GDAS24). There are relatively few high channel count receivers that are capable of time-series acquisition.

In a DAS, the quality and parameters of the IP measurement depend less on the receiver than on the perturbation source and the post-processing method. The source may fundamentally be configured as time-domain or frequency domain, usually with a square waveform in either case, and may be imposed using systems with signal strengths that vary from a few 10's of watts to 100 kW. For IP, high current > 1 A is desirable. And some systems can deliver 100 A. Signal processing can occur in the time-domain (referred to as 'binning and stacking') or the frequency domain (FFT). FFT provides for a more sophisticated calibration and signal extraction capability. In either case, a typical DAS will use at least one receiver channel to monitor and record the current. This ideally permits deconvolution of the signal at every receiver sampling point.

Magnetotellurics

For a DAS capable of MT, the sampling rate and sensors should cover a broad-band of perhaps 100 seconds to 10 kHz, although systems limited to 250 Hz upper end may practically be coupled with a deep-search DC system.

Robust, referenced processing (Egbert and Booker, 1986) is necessary and often extremely helpful in a near mine or culturally noisy environment. Using robust processing methods, MT resistivity can outperform DC resistivity even at shallow depths.

The 2D AMT acquisition method depends heavily on the principals of the EMAP method (Torres-Verdin and Bostick, 1992). A typical EMAP deployment does not include vertical coils (i.e. tipper is not available) and the number of cross-line electric field sensors (Ey dipoles) may be limited. MIMDAS, for example, typically deploys a single Ey and TITAN 24 typically deploys half as many Ey's as in-line (Ex) dipoles (e.g. 12-13 Ey's when 24 Ex's have been deployed). Similarly, for both systems, a single set of coils is deployed for the entire survey line.

For 2D surveys, 2D MT inversion methodologies such as the concepts of transverse electric (TE) and transverse magnetic (TM) modes and components are invoked. For 3D surveys, full-tensor inversions are more common.

DIGITAL SIGNAL PROCESSING (DSP)

DC Resistivity and IP

The Quantec IP acquisition system is a hybrid frequency- and time-domain system. A full-duty (frequency-domain) square wave is transmitted and data are received as time-series. The transmit frequency and receiver sampling rate are tuned to the ambient environment: For example, in a 60 Hz environments, the usual transmit frequency is 30/256 Hz and the time-series is sampled at 240 sps. Both transmitted and received signals are recorded as digital time-series.

To facilitate removal of EM coupling, the IP signal is evaluated using a (time-domain) half-duty square-wave model and the reported result is extracted from the decay curve at very late time (usually 0.8 seconds after turnoff through 0.2 seconds before turn-on). To provide a decay-time independent IP parameter that is also consistent with industry-recognized units, the reported units are phase in mrad.

A typical transmit contains 40 half-cycles, each lasting about 4 seconds, so the typical transmit period is about 2 minutes and 40 seconds.

Processing and QC include visual review of the time-series, manual adjustment of the time-window if necessary to avoid particularly noisy data, automated stacking with many configurable parameters, Fourier analysis, finite impulse response (FIR) filters for ambient power-line frequencies if necessary and iFFT to time-domain for decay representation.

The specific procedure is as follows:

1) Resample the current or response time-series as may be necessary (e.g. for ORION 3D which receivers are sampled at 1000 sps)
2) First pass sub-set stack of the time series
    a. To reduce long period oscillation
    b. Stack is based on ½ periods of the transmitter. The typical 'stack depth' is 5 half-periods.
        i. Use an overlapped, weighted (Halverson) strategy
            a. E.g. 1, -2, 1
        j. The typical result for 20 cycles is about 12 half-period groups
3) FFT

a. Apply calibrations to adjust for sensor impedance, sampling rate and logger characteristics (including gain).
b. Use a current and response transfer function to obtain V/I as in-phase and quadrature

4) Second pass stack
a. Use an error-weighted stacking strategy
b. Errors are managed using In-phase, quadrature or modulus parameters of a given harmonic (usually the quadrature of the 1st harmonic)
c. Apply robust outlier rejection

5) Isolate the fundamental and odd harmonics of the transmit and send this to the next stage of processing
6) Generate a finite impulse response (FIR) filter to roll-off at the power-line frequency
7) Generate a Sigma-Delta filter based on the Nyquist frequency of the sample rate to soften any digital noise and reduce singularities
8) Generate full- and half-duty waveform functions
9) Apply 6,7 and 8 to 5, then reverse FFT back to time domain
10) Calculate Vp from the full- duty cycle waveform
11) Calculate IP decay as chargeability from the half-duty cycle waveform
12) Calculate a late-time average chargeability for reporting
a. The ideal start-time is the earliest time for which EM coupling has died out. For a typical ~.1 Hz waveform Quantec usually uses 0.8 s
b. The ideal end-time is the latest time that is minimally affected by the filtering.
c. Taper the window to further reduce the impact of the filtering.

13) Scale the chargeability to phase
a. A linear scale is derived from the averaging-window and the Halverson-Wait half-duty model.
b. Use these 'standard' Halverson-Wait spectral parameters:
i. volume loading - 0.125 (chargeability equivalent of 0.5 mV/V)
ii. rValue - 1.0
iii. kValue - 0.2

The intention is that Quantec's TITAN 24 phase units then equate to a frequency-domain based phase measurement with minimal EM coupling (due to the late-time time-domain IP extraction). One caveat is that linearity of the Phase / Chargeability relation is predicated on a small fraction percent of sulphide (~ 5%), small grains and a regular distribution.

Magnetotellurics

The time-series is digitized at several sampling rates that depend on the sensors attached and the targeted spectral composition. Typical sampling rates for TITAN 24 are 48 kHz, 12 kHz and 100 or 120 Hz depending on powerline environment. For ORION 3D, a sampling rate of 1000 Hz is typical.

Time series data are calibrated and may be scrubbed for powerline frequencies, (Larsen et al 1996), then robust processing (e.g. Egbert and Booker, 1986) is used to extract the MT spectra. There are many fine and other darker arts to this process. Ultimately, the data are reviewed for quality, which also takes a high degree of skill and knowledge.

IMPROVEMENTS TO THE DAS & DSP

The SPARTAN MT connection

TITAN 24 relies on a LAN cable link. On the one hand, this permits real-time evaluation of the data, on the other hand this limits deployability and ultimately, channel count. The LAN permits accurate synchronization between the various receiver channels and the current. In order to run autonomous receivers, time synchronization is required. GPS clocks provide the required accuracy. Quantec's SPARTAN MT loggers use GPS time-synchronization. In 2007, Ken Nurse configured Quantec's processing software to manage GPS-stamped time-series for IP processing. This was the beginning of ORION 3D. The first ORION 3D survey was performed in 2007 in Nevada.

The RT-160's

The original ORION 3D survey was performed using loggers having a maximum sampling rate of 1000 sps. This limits the availability of AMT to 250 Hz upper frequency. New autonomous, GPS time-stamped loggers were developed and first deployed in 2012 that are capable of the full TITAN 24 acquisition band including up to 48 kHz sampling rate.

Improved calibrations

Since 2009, Quantec has internally calibrated magnetic field sensors. This is required because most manufacturers either do not calibrate sensors, or do not provide a broad-band calibration. Quantec's calibration uses a consistent environment, a magnetically shielded room and consistent standards such that sensors may be chosen to optimize responsiveness at particular bands, then combined to create optimal broadband responses, including that sensors from different manufactures may be combined.

Building Dipoles

In 2015 the ability to combine at the time-series level contiguous dipoles was developed. The tool is useful to build large dipoles to improve sensitivity at depth (Loke (1996-2014). It is also useful to augment coupling by, for example, building diagonal dipoles in a 3D survey, and it is useful for QC in 3D surveys. In a 3D survey with contiguous orthogonal dipoles, square 'loops' of various sizes may be traced. Any loop may be developed short one

last dipole length, such that data for that dipole position may be calculated to provide a comparison with the measured result at that location. We have found that such dipoles may be built over km distances and close within a few percent, which provides an excellent QC parameter. If a mismatch occurs, smaller and smaller loops are calculated until the problem dipole is identified.

This tool is also useful to calculate, for example, pole-dipole responses from pole-pole data.

And this tool may be used to combine two pairs of 'L'-shaped, contiguous dipoles into a '+' shape for a superior MT product from an ORION 3D survey (Figure 1).

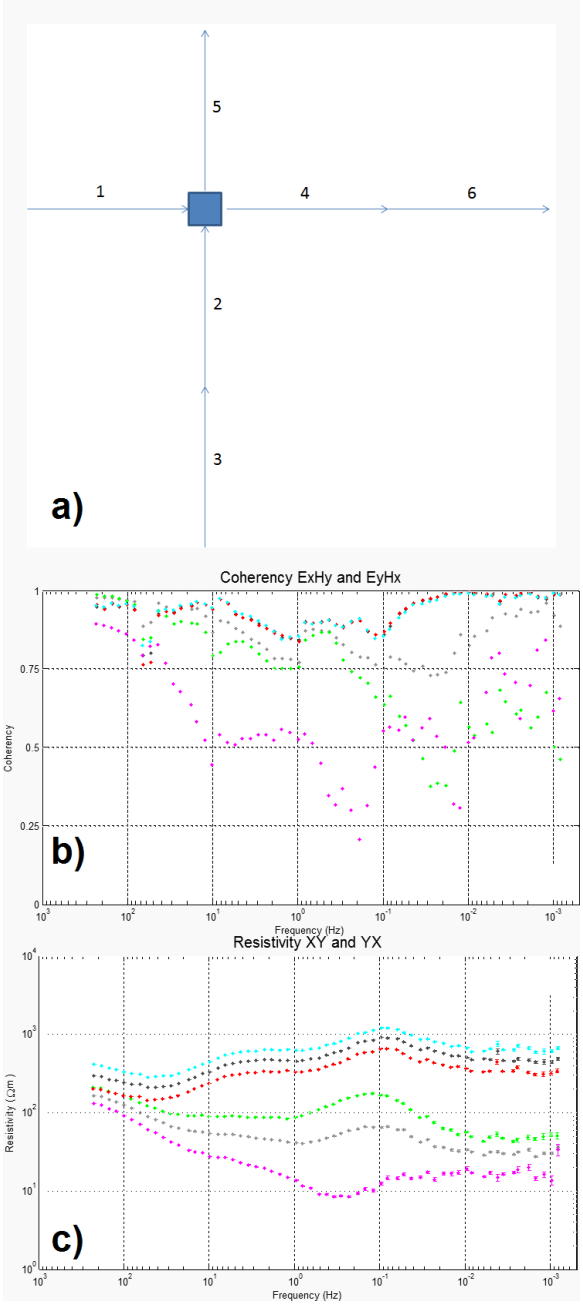

Figure 1: a) Typical Orion logger layout with dipole numbers; b) natural field (MT) coherency of local magnetic and electric fields; and c) MT resistivity vs frequency curves. XY modes are shown in blue, black and red; YX modes are shown pink, grey and green. Blue and pink correspond with MT calculated from dipoles 1 and 2, red and green correspond with MT calculated from dipoles 4 and 5 (both 'L's) and black and grey correspond with MT calculated using crossed dipoles built from 1 and 4; and 2 and 5.

Full versus Half duty

Some operators routinely acquire half-duty DCIP data. Figure 2 provides a comparison indicating the superiority of full-duty data collected with a DAS system; however, it

is occasionally useful to acquire half-duty data (e.g. the primary use for half duty data is that a half duty cycle puts less strain on the transmitting equipment). However, with new transmitter systems becoming available that are capable of transmitting more current into a half duty waveform, the signal advantage may improve.

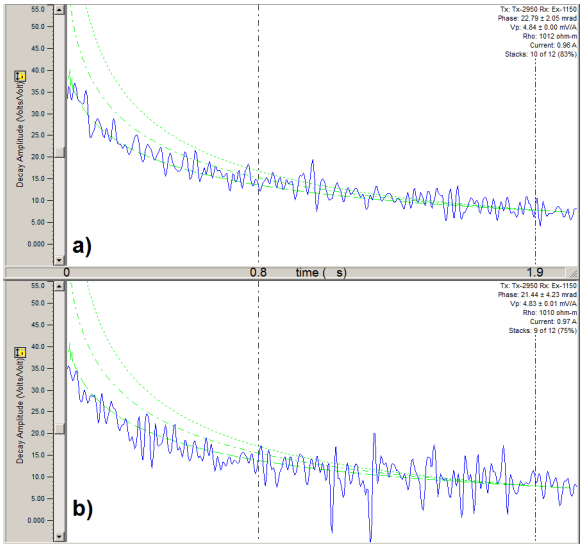

Figure 2: showing a long offset (1.8 km, n=18) IP decay for a) full duty and b) half duty. The dashed vertical lines at .8 and 1.9 s indicate the IP signal extraction time-range or 'window'. The green curves are idealized Halverson-Wait IP decays based on the late-time result and 'usual' parameter ranges. In production, they are used as QC guides. Phase results are 22.8 +/- 2 mrad at full duty and 21.4 +/-4 mrad at half duty. So errors are half as large and the H-W QC curves provide a visual aid that shows the shape of the decay is better behaved. These comparative results are typical.

Telluric Cancelation

The telluric cancelation method was proposed by Anaconda (Halverson, 1967). The method has been conceived using remote dipoles, remote coils, comparative evaluation of on-line time-series, and MISO-coherency analysis of remote sensors. Since stacking mitigates HF noise (and remote sensors may be too far away to be measuring the same HF signals), the method targets frequencies near the transmitter fundamental. The method requires a 'clean' remote that does not detect any IP signal, the location of which may necessarily be many 10's of km distant. The 'MIM' method (Rowston et al, 2003) requires the measurement of MT and therefore coils and at least one 'Ey' on the survey line.

Quantec has developed software for both the 'MIM' method (Figure 3) and a single-coil method that both produce similar results (~5-10% advantage) in the presence of certain telluric noise. Since this certain telluric noise is occasional, it has been our experience that TC generally adds only a small incremental value.

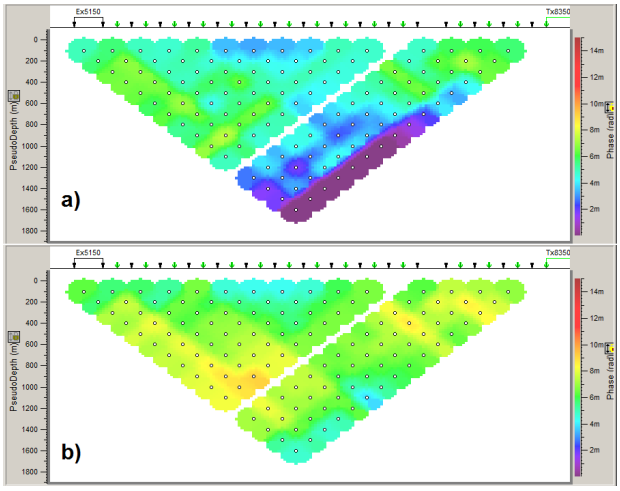

Figure 3: showing a Pseudosection of IP phase data a) before telluric cancelation and b) after TC.

PP2PDP

It is possible to calculate PDP data from PP data. We have use the built dipole tool and TITAN 24 time series to demonstrate that the built PDP data is noisier than acquired PDP.

Sampling rate tests

For FFT processing, sampling rates lower than 2x the powerline frequency will produce inferior 'hybrid' time domain results because fewer harmonics are available to the FFT. However, conversely, there seems to be little advantage to faster sampling rates until the threshold is past where actual frequency domain phase may be sampled (3000 sps for a 0.1 Hz transmit). Ideal frequency domain processing could be augmented if data storage, processing, management and harvest permitted much faster sampling rates (120 ksps).

Joint Inversion of DCIP and MT

Joint inversion of MT and DC (e.g. Wannamaker, 2007) combines the high shallow resolution of DC with deep investigation of MT to provide a coherent and complete resistivity section from surface to depth.

Ad hoc data improvements

When data are collected as raw time-series, it is possible to revisit the processing and continue to improve results long after the acquisition has been performed. Figure 4 shows the reduction of noise in an IP data-set that was due to a nearby pipeline protected using impressed current cathodic protection (ICCP). The noise severely affected the IP decay curves and IP results (Figure 5). The improved results were achieved after a concerted series of

trials including frequency domain filtering and signal isolation in raw time series. The signal isolation proved the most effective.

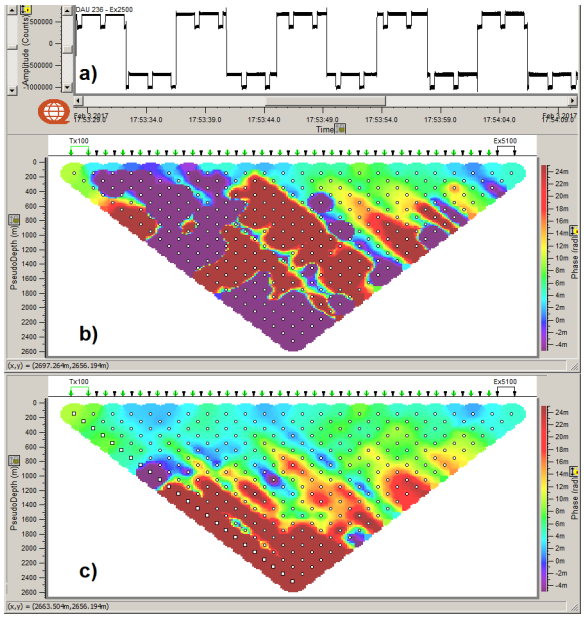

Figure 4: showing a) time-series affected by the ICCP noise, and pseudo-sections b) before noise removal and c) after noise removal.

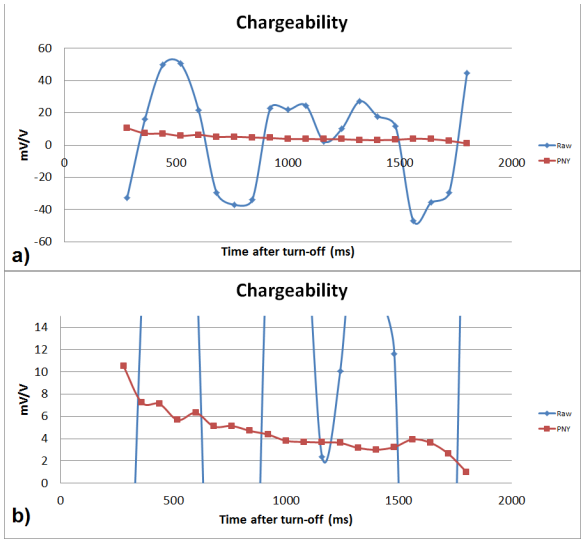

Figure 5: showing IP decay curves RAW before noise removal and after noise removal (PNY). Part (a) zoomed to the RAW scale and (b) zoomed to show the decay after noise reduction.

3D

The availability of 3D inversion software revealed weaknesses in conventionally acquired data. First, depending on line separation, but certainly for common line separations of 200 and 400 m, a typical acquisition of n = 6 and 50 m dipoles does not penetrate to sufficient depth to permit refined model development between the survey lines. Even at n = 10 and using a remote pole (PDP), the depth of investigation (and correlatively the cross-line investigation) is limited to less than 200 m. By providing exceptional depth of investigation (350 m at n = 20) a 2D DAS system provides an immediate improvement. However coupling with targets remain reliant on the 2D paradigm.

Improved '2.5D' coupling may be provided by offsetting the transmitter. In this case, two or four or even more receivers may be deployed on parallel 2D lines. Then when a parallel line of transmit poles is run 'up the middle' on a central line some cross-line investigation is made available to the inversion code. To perform this work, high channel-count receivers (or a distributed array) are vastly more efficient than moving 10-channel receivers around (or trying to deploy a large number of 10-channel receivers). A significant flaw is that shallow information may be compromised by null-coupling. In this central transmit configuration, when the transmitter and receiver are closest, the in-line receiver is null-coupled with (broadside to) the transmit pole.

The null-coupling problem may be solved by deploying orthogonal dipoles at each receiver station. While such a deployment is conceptually complicated with a high channel count receiver, a distributed array of low channel count receivers makes the deployment conceptually easy. All that is required is a very large quantity of autonomously operating (or wireless) distributed receivers.

An 'ultimate' refinement in 3D acquisition might be achieved by locating electrodes underground or in boreholes. This is not uncommon in smaller-scale environmental work.

For MT, there is a significant advantage to full tensor 3D inversion because it does not require 2D assumptions and artificial mode separation.

CONCLUSION AND A FORWARD LOOK

DAS systems are the demonstrated standard for deep search electrical mapping. The systems vastly outperform conventional surveys, particularly when DSP using FFT is included. However there is room for continued improvement. Some examples include: EM coupling and spectral analysis, use of subsurface electrodes, new noise mitigation such as wavelet analysis, time lapse monitoring, joint inversion, and incorporation of a distributed transmitter.

Fullagar et al (2000) introduce half-space modeling for removal of EM coupling in the time-domain while Routh and Oldenburg (2001) demonstrate similar techniques for the frequency domain. LaBrecque et al (2010) followed up with joint inversion for IP and EM coupling. Zhdanov 2008 introduces the GEMTIP

formulation that further integrates EM and IP for the purposes of both separation of EM coupling effects and mineral identification. Macnae (2016) describes how airborne IP is insensitive to the electro-chemical effects of economic mineral IP targets due to high base frequency, but very sensitive to 'Maxwell-Wagner' effects due to ionic fluids. This work on integrating EM, galvanic resistivity and IP will continue to improve the model and improve pertinent signal extraction.

Already, joint inversion of MT and DC is available. Further improvements in joint inversion methodology will integrate more diverse methods and help refine targeting. 3D visualization will improve.

Webster and Wondimu (2013) showed the value of adding subsurface electrodes. Employing borehole electrodes and performing electrical resistivity tomography including time-lapse tomography has become a usual practice in the environmental engineering business (e.g. Power 2014). It is expected that sub-surface electrodes may play an important role in certain near-mine, deep or high infrastructure environments.

High-channel counts using autonomous receivers will continue to evolve as the preferred methodology because this deployment can so flexibly accommodate obstacles, provide omnidirectional coupling for excellent resolution, and provide long offsets for excellent depth of investigation. Noise at long offsets is a factor. Time-series acquisition and DSP likely provide the solution. Deo and Cull (2016) explore wavelet processing as a potential new methodology and highlight the importance of time-series acquisition so that raw data are available as improved processing becomes available. It is likely underground deployment of electrodes will evolve and migrate into new practice of the mining business.

Similarly, time-lapse monitoring may translate into better management of leach and waste rock piles. Integration of techniques will improve.

Can we distribute the transmitter? Parra and Owen (1990) explored the use of multi-source arrays to focus exploration to depth, and at least one group (MPT, 2012) is exploring a distributed 'transceiver' concept in their acquisition system design and inversion codes.

REFERENCES

1967 SEG Mining Geophysics, Volume II Theory.

Bartel, L, Jacobson, R, 1987 Results of a controlled-source audiofrequency magnetotelluric survey at the Puhimau Thermal Area, Kilauea Volcano, Hawaii

Bleil, D, 1953, Induce Polarization: A method of geophysical prospecting: Geophysics (18) No. 3 pp.636-661

Bournas, N, Thomson D, 2013 Delineation of a porphyry copper-gold system using 3D DCIP, CSAMT and MT: KEGS symposium PDAC Toronto

Cagniard, L, 1953, Basic Theory of the Magneto-telluric method of Geophysical Prospecting: Geophysics 18, No. 3, pp. 605-635

Collins S, White R, 2003, Case histories in the use of three dimensional inversion of induced polarization and resistivity surveys, ASEG Geophysical Conference, Adelaide

Deo, R, Cull, J, 2016, Denoising time-domain induced polarization data using wavelet techniques: Exploration Geophysics (47) pp 108-114

Dey A, Morrison H.F, 1979 Resistivity modeling for arbitrarily shaped three-dimensional structures, Geophysics (44) No. 4 pp 753-780

Egbert, G and Booker, J, 1986, Robust estimation of geomagnetic transfer functions: Geophys. J. R. astr, Soc. (87) pp 187-194

Fullagar, P., Zhou, B, Bourne, B. 2000, EM-coupling removal from time-domain IP data

Gharibi, M., Killin, K., McGill D., and Henderson W, 2012, Data redundancy in an omnidirectional 3D DC resistivity dataset: International geophysical Conference and Exhibition, Istanbul

Goldie M, 2007, A comparison between conventional and distributed acquisition induced polarization surveys for gold exploration in Nevada: The Leading Edge PP 180-183

Goldstein, M, Strangway, D, 1975, Audio-frequency Magnetotellurics with a grounded electric dipole source: Geophysics (40< No. 4 pp 669-683

Hallof, P. 1974, The IP phase measurement and inductive coupling, geophysics (39) No. 5, pp 650-665

Halverson M., 1967, A look at dispersion and induced polarization using the phase angle concept: Proceedings of the symposium on induced electrical polarization, February, 1967, UC Berkeley.

Halverson M, Zinn, W, McAllister, E, Ellis, R, Yates, W, 1981, Assessment of results of broad-band spectral IP field tests: in Advances in induced polarization and complex resistivity January 1981 U. Arizona Workshop

Kingman J, 1994, Digital signal processing approaches to interpreting induced polarization data: John S. Sumner memorial international workshop on IP in mining and the Environment, Tucson AZ

Larsen, J. Mackie, R, Mansella, A, Fiordelisi, A, Riven S, 1996, Robust smooth magnetotelluric transfer functions: Geophys J. Int (124) pp 801-819

Loke, D, 1996-2014, Tutorial: 2-D and 3-D electrical imaging surveys, http://www.geotomosoft.com

Loke, M, Frankcombe K, Rucker D, 2013, The inversion of data from complex 3-D resistivity and I.P. surveys: ASEG-PESA 2013, Kilbourne

LaBrecque D, Casale, D, Adkins, P, 2010 Join t modeling of EM coupling and spectral IP data: Proceedings of SAGEEP, EEGS

Macnae. J, 2016, Developments in airborne IP, KEGS special lecture, Toronto

Multi-phase Technologies, 2012, Multi-source transceiver brochure. http://www.mpt3d.com

Nyquist J, 2005, Improved 3D pole-dipole resistivity surveys using radial measurement pairs: geophysical Research Letters (32)

Oldenburg, D, Li, Y., 1994, Inversion of induced polarization data: geophysics 59, pp 1327-1341

Parra, J, Owen, T, 1990, Synthetically focused resistivity for detecting deep targets: In SEG Geotechnical and Environmental Geophysics, Volume III Geotechnical, 1990, Ward, S. Ed. Pp 37-50

Pelton W, Ward S, Hallof P, Sill W, and Nelson P, 1978 Mineral discrimination and removal of inductive coupling with multi-frequency IP, Geophysics 43 No 3, pp 588-609

Power, C, 2014, Electrical resistivity tomography for mapping subsurface remediation: University of Western Ontario Ph.D. Thesis

Rowston P, Busuttil, S, McNeill, G, 2003 Cole-Cole inversion of telluric cancelled IP data: ASEG Conference, Adelaide.

Routh, P, Oldenburg, D, 2001 Electromagnetic coupling in frequency-domain induced polarization data: a method for removal, Geophysical journal int. (145) 59-76

Sheard N, Ritchie, T, Kingman, J. and Rawston, P, 1998, MIMDAS - A new direction in geophysics: 13th ASEG Conference and Exhibition

Seigel H., 1959, Mathematical Formulation and Type Curves for IP: Geophysics 24 (3) 547-565

Slater L, Lesmes, D, Sandberg, S, 2000, IP interpretation in environmental investigations: Proceedings of SAGEEP, EEGS

Strangway, D, Swift, C, Holmer R, 1973, The application of audio-frequency Magnetotellurics (AMT) to mineral exploration: Geophysics (38), No. 6 pp 1159-175

Torres-Verdin, C, Bostick, F, 1992, Principles of spatial surface electric field filtering in magnetotellurics: Electromagnetic array profiling (EMAP): Geophyiscs (57) No. 4 pp 603-632

Tunser, V, Unsworth, M, Siripunvaraporn, W, Craven J, 2006, Exploration for unconformity-type uranium deposits with audiomagnetotellurics data: A case study from the McArthur River Mine, Saskatchewan, Canada: Geophysics (71) No. 6 pp B201-B209

Wannamaker, P, Doerner W, 2002, Crustal structure of the Ruby Mountains and southern Carlin Trend region, Nevada, from Magnetotelluric data: Ore Geology Reviews (21), pp 185-210

Wannamaker, P, Stodt, J, Rijo, L, 1987, A stable finite element solution for two-dimensional Magnetotelluric modelling: Geophys, J.R. ast. Soc. No. 88 pp 277-296

Wannamaker, P, 2007, Joint Inversion of TITAN-24 MT-PDP array data from the Kidd Carnegie project, Ontario: Vismand Exploration submission to Ontario MNDM available at http://www.geologyontario.mndmf.gov.on.ca/mndmfiles/afri/data/imaging/20000005997//20008528.pdf

Webster B., Wondimu H, 2013, Copper delineation with Clarity3D DSIP/Resistivity system: KEGS symposium PDAC Toronto

Webb D, Rowston P, McNeil G, 2003, A comparison of 2D and 3D IP from Copper Hill NSW, ASEG Geophysical Conference, Adelaide

Zhdanov, M., 2008, Generalized effective-medium theory of induced polarization: Geophysics (73) No. 5 F197-F211

Zonge, K. Sauck W, Sumner, J, 1972, Comparison of Time, Frequency and Phase measurements in induced polarization, Geophysical prospecting (20),, 626-648